

LHCb-2007-082  
11 April 2008

# VELO Module Production - Vacuum Tank Tests

## LHCb Technical Note

Issue: Draft  
Revision: 4Reference: LHCb 2007-082  
Created: 10<sup>th</sup> October 2006  
Last modified: 11<sup>th</sup> April 2008Prepared By: **LHCb Liverpool VELO Group\***  
Author: **G.L. Casse, D. Hutchcroft, D. Jones**  
Editor: **G.D. Patel**

### Abstract

This document describes the procedure for the burn-in of the completed module in the vacuum tank.

### Document Status Sheet

<b>1. Document Title: VELO Module Production - Vacuum Tank Tests</b>			
<b>2. Document Reference Number: LHCb-2007-082</b>			
<b>3. Issue</b>	<b>4. Revision</b>	<b>5. Date</b>	<b>6. Reason for change</b>
Draft	1	10 <sup>th</sup> October 2006	First version
Draft	2	28 <sup>th</sup> January 2008	Revision to simplify the discussion on procedures
Draft	3	5 <sup>th</sup> March 2008	Addition of results and conclusion, streamlining of text
Draft	4	11 <sup>th</sup> April 2008	Add Ref [6] as Appendix

\*Liverpool VELO Group: A.A.Affolder, T.J.V.Bowcock, J.L.Carroll, G.L.Casse, P.A.Cooke, L.Dwyer, K.Hennessey, T.Huse, D.Hutchcroft, D.E.L.Jones, M.Lockwood, D.Muskett, G.D.Patel, K.Rinnert, T.Shears, N.A.Smith, G.Southern, P.Sutcliffe, M.Tobin, P.R.Turner, M.Whitley, M.Wormald

---

## Table of Contents

<b>1. Introduction .....</b>	<b>1</b>
<b>2. Equipment.....</b>	<b>1</b>
2.1. Vacuum Tank and Systems .....	1
2.2. Cooling Systems .....	3
2.3. Temperature Monitoring .....	3
2.4. Thermal Camera.....	3
2.5. Low Voltage Systems.....	4
2.6. High Voltage Systems.....	4
2.7. Module position monitoring.....	4
2.8. DAQ and TELL1 .....	5
2.9. Software.....	6
2.10. Modules and Kapton cables.....	6
<b>3. Procedure .....</b>	<b>6</b>
3.1. Burn-in Cycle.....	6
3.2. Logging.....	6
3.3. Noise Rates .....	7
3.4. Thermographs .....	8
<b>4. Results .....</b>	<b>8</b>
4.1. Mechanical Displacements.....	8
4.2. Electrical Faults.....	9
4.3. Thermal Performance.....	9
<b>5. Conclusions .....</b>	<b>10</b>
<b>6. References .....</b>	<b>11</b>
<b>Appendix A : Summary of Thermal and Mechanical Measurements.....</b>	<b>12</b>
<b>Appendix B : Reference [6] Thermal Test of VELO module.....</b>	<b>13</b>

## 1. Introduction

The burn-in system described here is the one at the Department of Physics at the University of Liverpool used during the production of the LHCb VELO modules

The burn-in system at Liverpool was set up with the following aims;

- To test modules for basic functionality
- To test modules in an environment that attempts to mimic the situation of the final experiment
- To gauge physical properties of modules; such as variations in shape due to differential thermal expansion
- To gauge the thermal properties of the module
- To try and provoke early failure before module shipping by providing thermal cycling and a short burn-in test
- To check that the module fulfils a set of qualification criteria and to reject those that do not pass these tests

## 2. Equipment

The system is housed in clean room conditions (class 1,000) and consists of the following major systems:

- A vacuum tank with two pumps for evacuating the tank
- A mount for the module inside the tank with feed through for the power supplies and readout cabling
- Two repeater boards on the outside of the tank feeding 10m cables to the DAQ system
- Two low voltage power supplies for powering the module
- Two high voltage Source Measurements Units (SMU's), one for each sensor
- A CO<sub>2</sub> based cooling system which cools the module inside the tank
- A Thermal camera
- A Capacitance meter
- A DAQ system based on the TELL1[1, 2] system used in the LHCb experiment

### 2.1. Vacuum Tank and Systems

A large cylinder forms the main body of the tank; vacuum system connections are made to this cylinder and the opening for insertion of modules is at one end of this cylinder. Fixed either side of this main cylinder are two cylinders which form a cross shape. The two cylinders have germanium windows, aligned perpendicular to the sensors surface, with mounting holes for placing the thermal camera. The vacuum tank is shown in Figure 1. The two windows allow thermographs to be taken of both sides of the hybrid during a burn-in test. A drawing of the vacuum tank that shows the position the module is shown in Figure 2.

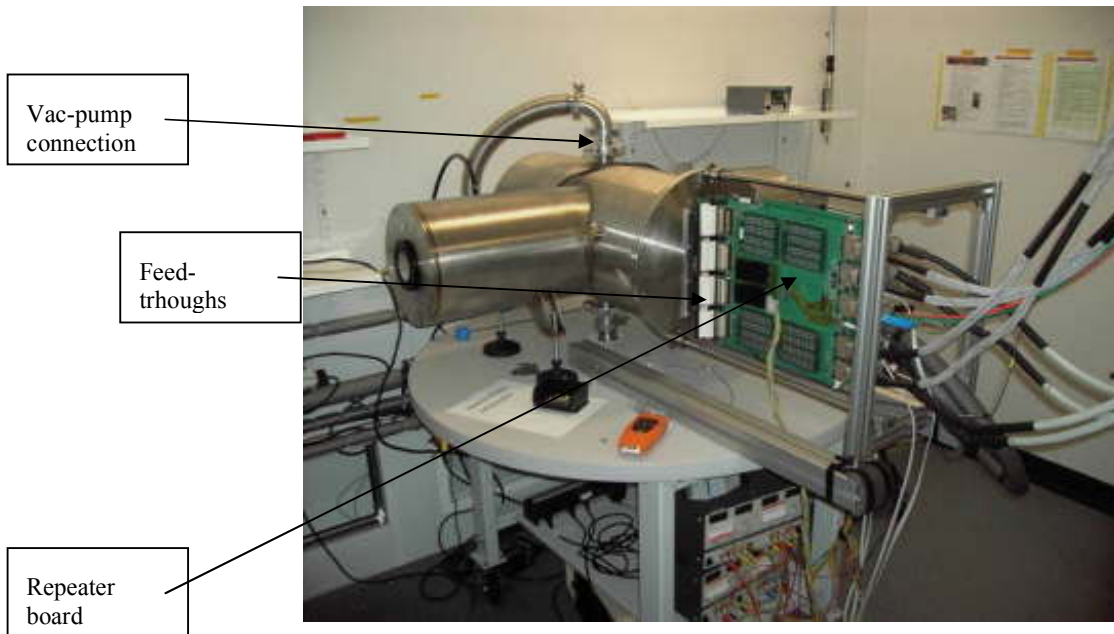


Figure 1: Vacuum tank

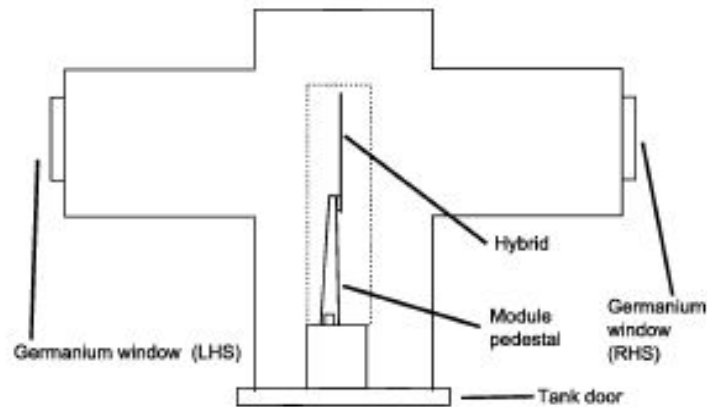


Figure 2: Schematic cross-section of the vacuum tank

The vacuum system (Fig. 1), is equipped with a scroll pump used to reduce the pressure from atmospheric to about 0.2 mbar and a turbo pump (switched-on in parallel to the scroll pump below this value) to obtain the final pressure. Associated with the vacuum system are the air admittance valves, three pressure gauges and two low pressure vacuum Penning gauges.



Figure 3: Vacuum pump system

## 2.2. Cooling Systems

The electronics on the modules dissipates a significant amounts of heat in normal operation, particularly from the 16 Beetle [3, 4] front end chips on each side of the hybrid, that dissipate about 20W of power. A CO<sub>2</sub> based cooling system is used to maintain the module at its nominal operating temperature (below -7°C). This is a simplified version of the cooling design designed for the VELO detector.

High pressure gaseous CO<sub>2</sub> is provided by a bottle. The gas is allowed to expanded and cool after a flow control valve which causes it to liquefy before passing into the tank. Inside the tank the liquid CO<sub>2</sub> flows down a narrow aluminium tube to the module. The aluminium pipe is wound through five plates called cooling cookies where the liquid CO<sub>2</sub> partially evaporates, cooling the module. The CO<sub>2</sub> gas mixture goes through a flow control valve to adjust the flow rate and so the cooling efficiency on the module. The flow valve is manually adjusted to change the temperature of the module and therefore to perform the thermal cycling test. The cold gas is passed through a heat exchanger to pre-cool the incoming CO<sub>2</sub>. Finally the CO<sub>2</sub> is heated to room temperature and vented outside the building. A CO<sub>2</sub> concentration monitor is used to ensure that in the event of a leak personnel would be warned of increased CO<sub>2</sub> concentration in the confined space around the vacuum tank. The asphyxiation risk of CO<sub>2</sub> in the confined space requires that there are at least two people present at all times when the CO<sub>2</sub> is flowing.

The input and output pressure of the CO<sub>2</sub> and the flow rate of the CO<sub>2</sub> are monitored. There are 4 sensors measuring the temperature at different points in the CO<sub>2</sub> system.

The thermal contact between the cooling cookies and the carbon fibre of the module is made by a thermal compound which is supplied as sheets of thin flexible plastic/putty material. This is cut into rectangles that are placed between the cookies and the module. The cookies are then screwed to the module compressing the thermal compound. The material chosen for the burn-in tests can be removed with very little residue, in the final experiment a liquid is used between the cookies and the module that is then hardened in place. This material is very difficult to remove from the module and the cookies but provides a better thermal contact and is both vacuum and radiation tested. The material used in the burn-in has not been radiation tested and contributes significantly to the residual pressure in the vacuum tank.

## 2.3. Temperature Monitoring

The burn-in setup has a number of temperature meters that are manually logged (see 3.8). There are four four temperature sensors on the cooling system and four on the module itself (thermistors), namely two in the middle of the module next to the cooling block (one on each side) and two close to the readout chips on each side of the module.

## 2.4. Thermal Camera

The thermal camera setup consists of an infrared camera, a PC interface card and a laptop computer which runs the interface and control software. Both sides of the module can be viewed using the camera although

with only one camera this requires moving the camera to either side of the tank. The camera is mounted to a frame which is aligned with dowel pins and mounting bolts on either side of the tank.

Data are acquired by the cameras software and can be stored in a propriety format and also exported as a bitmap file. Using the thermal camera as a diagnostic tool is discussed under section 6.

## **2.5. Low Voltage Systems**

The Beetle chips on the module and the repeater board are powered from two Tandberg power supplies, which also monitor the current drawn by the system. All of the power and readout signals are provided to and read from the modules along a pair of Kapton laminated cables that pass through the end plate of the module (feed throughs).

## **2.6. High Voltage Systems**

The high voltage system provides the bias required to deplete the silicon sensors. A combined high voltage supply and current meter (SMU) is used to provide the potential difference and to measure the leakage current with nA precision. The unit allows, amongst other features, an over current protection limit to be set. One unit is used for each sensor.

The units allow IV curves to be produced by increasing the voltage in small steps and recording the leakage current at each point.

## **2.7. Module position monitoring**

The differential thermal expansion rates of the materials constituting a modules can mean that the hybrid shape changes as the modules temperature varies. The design is symmetrical so the expected deflections are small. The size of the deflections is monitored by a capacitance meter which measures the change in capacitance between a small fixed plate on the support and a flat copper sheet clipped to the hybrid between the cooling and the sensor, as shown in

. The change in capacitance is manually logged as the module is thermally cycled.

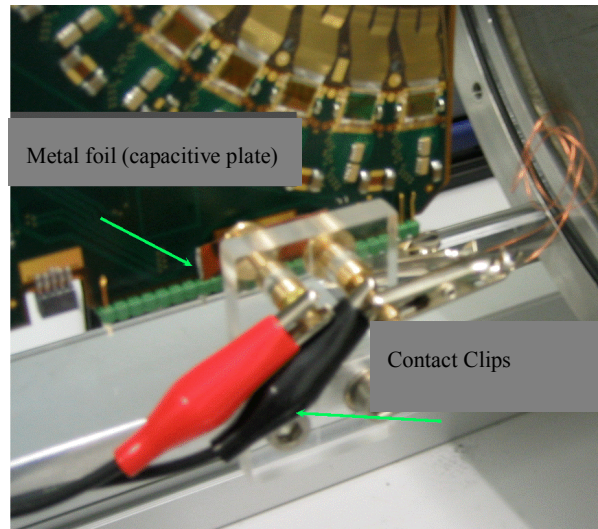


Figure 4: Capacitive module moment measuring system.

The relationship between the change in the capacitance and the amount of deflection was determined using a dial test indicator. The module was deflected manually normal to the hybrid face and the response of the 'clock' and LCR meter was recorded. As shown in Figure 5, it was determined that a change of capacitance of 1 fF corresponds to a 2  $\mu\text{m}$  motion of the hybrid perpendicular to its face.

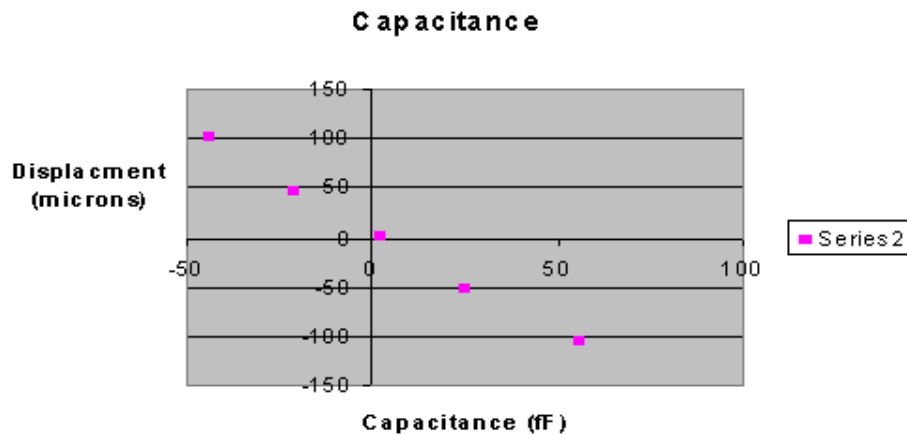


Figure 5: Displacement (in microns) of the module normal to the hybrid face as a function of the measured capacitance on the module position measuring system (in fF).

## 2.8. DAQ and TELL1

The DAQ system consists of the repeater boards, cabling, TELL1 and the related computing systems. The burn-in setup is a reduced slice of the real DAQ system that will be installed for the LHCb vertex detector in the experiment. Kapton cables from the module connect to the feed-throughs which route the lines to the repeater board. The repeater board is connected to the TELL1 via 4 sets of cables. One repeater board, cable set and TELL1 is required for each sensor; a module requires 2copies of this setup.

When the burn-in DAQ system, shown in Figure 6, was setup there was only one TELL1 available; it is used to readout both sides by swapping the two sets of four of cables at the TELL1. The repeater boards themselves required a small amount of modification to allow this operational mode.

The TELL1 board is connected to the desktop computer used to run the DAQ via an Ethernet connection. Control of the TELL1 board is possible by using a secure shell to log into the credit card PC (CCPC) mounted as a daughter board on the main TELL1 board. Using this connection the TELL1 can be initialised, reset and instructed to take data in an adjustable sized burst.

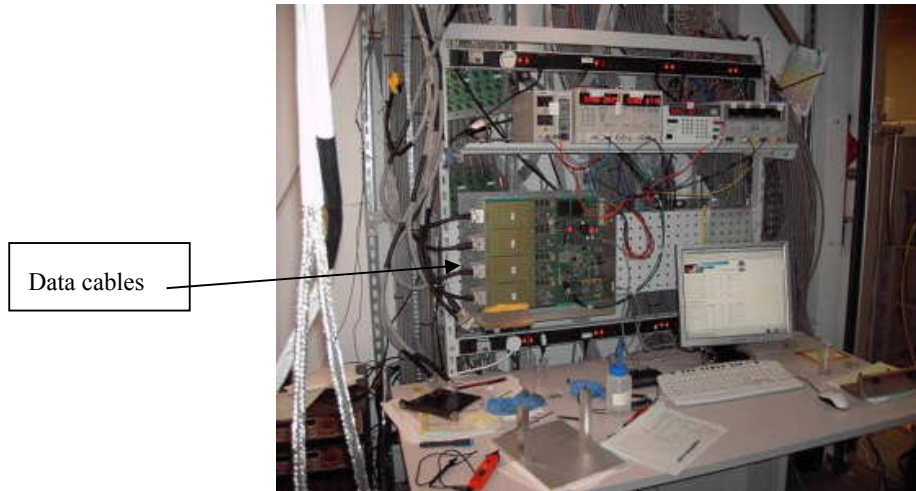


Figure 6: Picture of the Tell1 DAQ system

## 2.9. Software

The software used to acquire data from the VELO sensors resides on the CCPC (located on the TELL1 board) and a dedicated desktop PC, which is used to run the system and store the data. The desktop PC is also used to record the data into a spreadsheet that is manually logged from the various visual readouts on the setup. The analysis of the non-zero suppressed data is done on this computer using custom modules in the normal LHCb software framework[5].

## 2.10. Modules and Kapton cables

Usually modules that have been completed and have passed all the quality control checks, bar a final metrology and visual inspection, are tested in the burn-in system. Modules are paired with the set of four Kapton cables that will be used in the final experiment. A spare set of Kapton cables was also available for diagnosis purposes. A modified grounding strap used for testing is part of the burn-in setup, the modifications are to prevent it breaking when modules are repeatedly inserted or removed.

## 3. Procedure

### 3.1. Burn-in Cycle

The burn-in cycle involves two temperature cycles, between the lowest achievable with the CO<sub>2</sub> system (-25°C) and +35°C. The second cycle was added after a failure was observed in one of the first modules during a temperature cycle. During production the length of the burn-in cycle was reduced to increase module throughput.

### 3.2. Logging

During the burn-in procedure data logging is performed manually. A spreadsheet is used to record the following quantities;



- Time and date.
- Vacuum pressure.
- Capacitance of the monitoring foil to measure the displacement of the module.
- Module temperatures (four temperature readings of the thermistors located on the module).
- Cooling system temperatures (CO<sub>2</sub> input, output and heat exchanger).
- Cooling system input pressure and flow rate.
- Low voltage current.
- High voltage: voltage and leakage current for each sensor.
- Any additional text comments on the state of the burn-in.

Figure 7 shows the measured environmental quantities logged during a cooling cycle during the commissioning of the system.

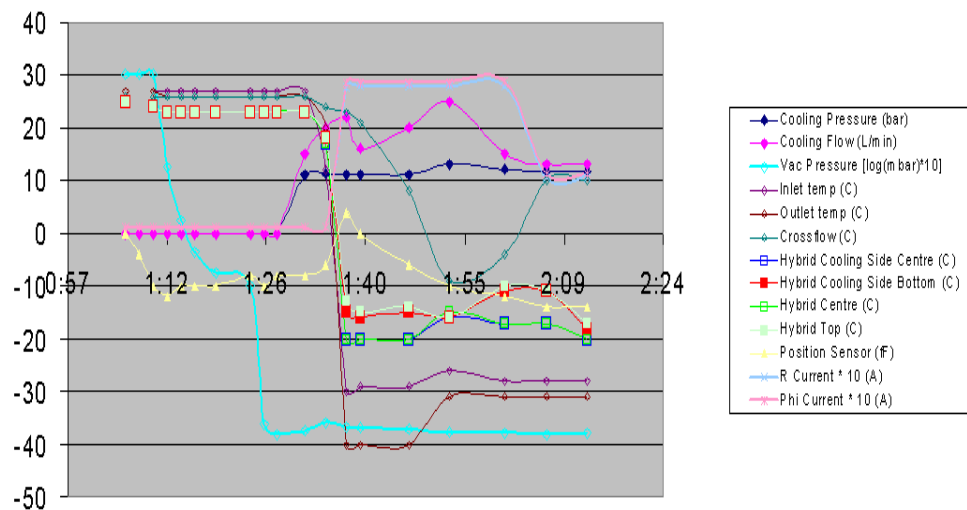


Figure 7: Measured environmental quantities during a thermal cycle

### 3.3. Noise Rates

Each module was tested in the dark with no external sources of injected charge at nominal operating environmental conditions, i.e. at about -18/-20 °C at the base of the hybrid and in vacuum. Under these conditions, noise data was taken with the Tell1 readout DAQ. The data was analysed with custom off-line software, which calculated the raw noise, the pedestal, and the common mode subtracted noise for the each channel. The data were then analysed to locate any channels with non-standard noise behaviour which could indicate faulty channels. The list of faulty channels was then compared to the bad channel lists previously generated by the laser test stand [5]. As the analysis program was over-efficient at indicating problem channels, the results were visually inspected by two physicists.

During the production run, various problems with the DAQ chain were encountered. The TELL1 cables were attached with a clip-on connector that turned out to be unreliable, which resulted in the cables partially falling out as the tank was moved. Additional problems were traced to bad contacts on the repeater boards that required resoldering. Finally, the internal connections between the long cables and their connectors failed initially at a high rate due to a very stiff outer sleeve. The cables were replaced eventually with units that had their sleeves stripped back from the connectors by 20cm; these new cables did not fail.

### 3.4. Thermographs

After data taking, thermographs of both the R-side and Phi-side of each module were taken under nominal operating conditions. The thermographs were an invaluable aid to locating shorts on the hybrids as hot spots and in qualifying the thermal continuity of the thermal pyrolytic graphite (TPG) core of the module. The temperature of the silicon sensors was ascertained by analyzing the thermographs using the thermal camera's software package. The absolute temperature requires the software to be calibrated for the emissivity of the material, hence only the fraction of the sensor without aluminium coating was correctly calibrated [6].

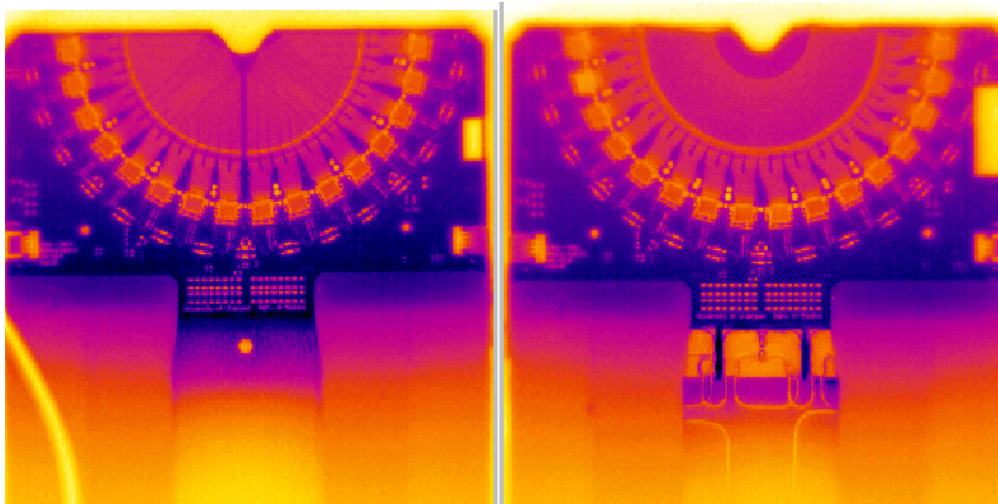


Figure 8: Thermographs of an R-side (left) and Phi-side (right) of VELO module with maximal cooling and the Beetle chips operational.

## 4. Results

### 4.1. Mechanical Displacements

Mechanical displacements of the modules were monitored throughout all cooling cycles using the variation of the capacitance of a foil mounted on the module relative to a facing pad fixed on the tank. A change of capacitance of 1 fF equates to a 2  $\mu\text{m}$  displacement of the hybrid perpendicular to its surface, as shown in Fig. 5. Figure 9 shows the measured maximal displacements of the modules as a function of test date. Early in the production (prior to October 2006), the measured deflection were larger than expected, with a mean of 69  $\mu\text{m}$  and a standard deviation of 42  $\mu\text{m}$ . The reason for the over-deflection was identified in small variations in the way the cable clamps were attached to the modules. Cable clamps [7] are used to relieve the force exerted by the kapton cables onto the hybrid when contracting during temperature cooling. Small differences in the location of the clamps lead to different push/pull action on the module as a function of the operating temperature. To solve the issue, marks were added to the cables (after October 2006) to indicate the correct (neutral) position of the cable clamps relative to the cables [7]. The measured deflection decreased appreciably with an average displacement of 31  $\mu\text{m}$  with a standard deviation of 35  $\mu\text{m}$ .

After the cable location marking, there were a few (3-5) tests with abnormally large deflections. It is assumed these large deflections were also caused by mis-clamping of cables. As the constraint system [8] reduces the importance of such deflections and as any re-test of a module would be extremely time-intensive (4-8 hours), it was decided not to re-do these measurements.

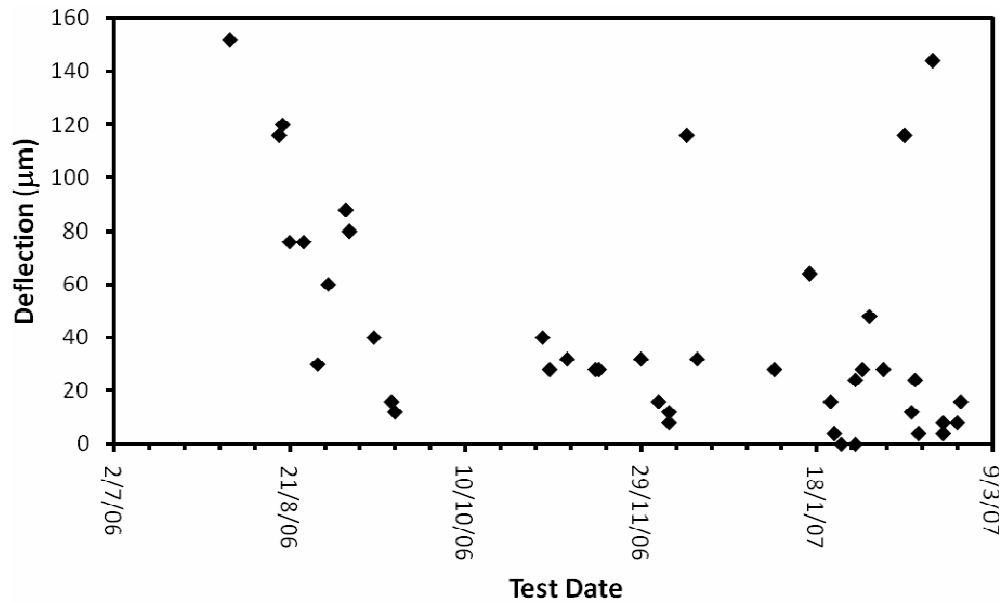


Figure 9: Measured mechanical deflection of modules vs. test date

## 4.2. Electrical Faults

The results of the electrical measurements are given in Ref. [5]. No additional opens, shorts, or low gain channels were found relative to the laser tests. This indicates that no failures of wire bonds or Beetle chips developed during the thermal cycling or data taking. The only additional faulty channels found were high noise channels. On average, 1.6 additional noisy channels were found during the vacuum tests. Many of these new high noise channels are probably false and caused by the lack of spill-over correction in the noise calculation for vacuum tank data. 0.58% of the channels in total were marked as faulty.

## 4.3. Thermal Performance

The thermal performance measurements are shown in Figure 10 and in appendix A. Of the 46 modules tested, 44 behaved as expected. With an average temperature between the inlet and outlet of the CO<sub>2</sub> coolant of -30.8 C°, the average temperature of the silicon sensors was measured to be -8.1 C°. The temperature difference between the coolant and the sensors has been shown to be smaller in the final installation. This behaviour is most likely due to the use of thermo-flow between the final cooling cookies and the hybrid (as described before) and due to having cold neighbouring modules in the final system. The average temperatures of the central and edge thermistors on the hybrids were -19 C° and -11.3 C° respectively.

Two modules were rejected as the temperature of the silicon was too high relative to the temperature of the base of the module when in operation. The thermographs revealed that there were discontinuities in the thermal profile of the hybrids that were apparently cracks in the pyrolytic graphite core. More detailed descriptions of the failed modules are given in the following sections.

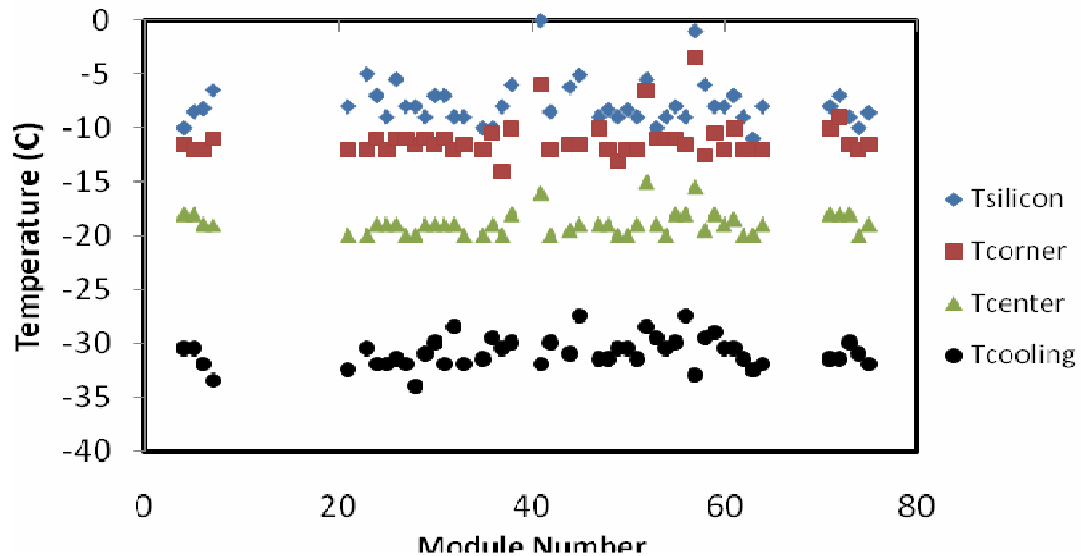


Figure 10: Summary of thermal measurements. Tcorner and Tcenter are the measurements of the thermistors on the hybrid. Tcooling is the average temperature of the cooling inlet and outlet.

#### 4.3.1. Module 41

Prior to shipment to CERN, this module had a normal cooling performance. On installation into the final system at CERN and in subsequent cooling tests, module 41 showed a worsening thermal performance. The module was removed and set to Liverpool for further study. Subsequent investigations at Liverpool confirmed the degraded thermal performance. The measured temperature at the central thermistors on the module had increased from  $-18\text{ }^{\circ}\text{C}$  to  $-16\text{ }^{\circ}\text{C}$ ; on the edge thermistors, the temperature increased from  $-9\text{ }^{\circ}\text{C}$  to  $-6\text{ }^{\circ}\text{C}$ . There was no discernable cause for the degrading thermal performance and the module was rejected.

#### 4.3.2. Module 57

Module 57 was failed as a result of vacuum tests performed at Liverpool. The module had poor thermal performance. The sensor temperature was  $7.1\text{ }^{\circ}\text{C}$  warmer than the average module. The central thermistors on the module nearest the cooling cookies were about 3.5 degrees warmer than other modules running under the same conditions. Furthermore, the edge thermistors located further up the module were 7.8 degrees warmer than average.

One indication of the cause of the thermal anomalies was the asymmetry of the measured temperature of the two edge thermistors, which were 3 degrees different. Closer inspection of the thermograph confirmed that a corner of the hybrid had an elevated temperature. This asymmetry in the temperature may be indicative of a cracked TPG core or other fault involving the substrate. Module 57 was terminated after these detailed investigations.

## 5. Conclusions

Each module was tested under approximately final operational conditions using the Liverpool vacuum tank system. During these tests, the electrical and thermal performances of the modules were measured and the mechanical displacements of the modules throughout the thermal cycles were monitored. The mechanical displacements were as expected when the module's cables were clamped properly. No Beetle chips failed during operation or during the thermal cycles. No additional opens, shorts, or low gain channels were found. A total of 2 of the 46 modules tested had degraded thermal performance relative to expectations and were rejected.

## 6. References

1. Haefeli, G. and others, The LHCb DAQ interface board TELL1. Nucl. Instrum. Meth., 2006. A560: p. 494-502.
2. Legger, F., et al., TELL1: Development of a common readout board for LHCb. Nucl. Instrum. Meth., 2004. A535: p. 497-499.
3. Agari, M. and others, Beetle: A radiation hard readout chip for the LHCb experiment. Nucl. Instrum. Meth., 2004. A518: p. 468-469.
4. Lochner, S. and M. Schmelling, The Beetle Reference Manual. LHCb Internal Note, 2006(105).
5. Rinnert, K., et al., VELO Module Production - Laser Test and Noise Analysis. LHCb Internal Note, 2007(083).
6. Oldeman, R., et al., Thermal test of LHCb VELO module 14 and a test of TPG inserts. See Appendix B.
7. Smith, N.A., et al., VELO Module Production - Cable Clamp Attachment. LHCb Internal Note, 2007(077).
8. Carroll, J.L., et al., VELO Module Constraint System. LHCb Internal Note, 2007(089).

## Appendix A : Summary of Thermal and Mechanical Measurements

Module	T <sub>center1</sub> (C)	T <sub>bottom</sub> (C)	T <sub>center2</sub> (C)	T <sub>top</sub> (C)	T <sub>input</sub> (C)	T <sub>out</sub> (C)	T <sub>silicon</sub> (C)	Max. Move. (μm)
21	-20	-12	-20		-32	-33	-8	30
28	-20	-12	-20	-11	-35	-33	-8	76
23	-20	-12	-20	-12	-31	-30	-5	76
24	-19	-11	-19	-11	-32	-32	-7	116
25	-19	-12	-19	-12	-31	-33	-9	88
26	-19	-11	-19	-11	-31	-32	-5.5	120
27	-20	-11	-20	-11	-31	-33	-8	152
29	-19	-12	-19	-10	-33	-29	-9	60
30	-19	-11	-19	-12	-28	-32	-7	80
31	-19	-11	-19	-11	-31	-33	-7	
32	-19	-12	-19	-12	-28	-29	-9	40
33	-20	-12	-20	-11	-31	-33	-9	40
35	-20	-12	-20	-12	-30	-33	-10	16
36	-19	-11	-19	-10	-28	-31	-10	12
37	-20	-14	-20	-14	-30	-31	-8	
38	-18	-10	-18	-10	-29	-31	-6	28
41	-16	-6	-16	-6	-32	-32		
42	-20	-12	-20	-12	-30	-30	-8.5	32
44	-20	-12	-19	-11	-31	-31	-6.2	28
45	-19	-12	-19	-11	-29	-26	-5.1	28
47	-19	-10	-19	-10	-31	-32	-9	32
48	-19	-12	-19	-12	-31	-32	-8.3	8
49	-20	-12	-20	-14	-31	-30	-9	32
50	-20	-12	-20	-12	-30	-31	-8.3	16
51	-19	-12	-19	-12	-31	-32	-9	12
52	-15	-7	-15	-6	-27	-30	-5.5	116
53	-19	-11	-19	-11	-30	-29	-10	64
54	-20	-11	-20	-11	-30	-31	-9	16
55	-18	-11	-18	-11	-29	-31	-8	4
56	-18	-12	-18	-11	-31	-24	-9	0
57	-16	-2	-15	-5	-33	-33	-1	
58	-20	-13	-19	-12	-30	-29	-6	0
59	-18	-11	-18	-10	-30	-28	-8	24
60	-19	-12	-19	-12	-30	-31	-8	28
61	-19	-10	-18	-10	-31	-30	-7	48
62	-20	-12	-20	-12	-31	-32	-9	28
63	-20	-12	-20	-12	-32	-33	-11	28
64	-19	-12	-19	-12	-31	-33	-8	116
71	-18	-10	-18	-10	-31	-32	-8	12
72	-18	-9	-18	-9	-31	-32	-7	24
73	-18	-12	-18	-11	-31	-29	-9	4
74	-20	-12	-20	-12	-30	-32	-10	144
75	-19	-12	-19	-11	-32	-32	-8.6	8
4	-18	-12	-18	-11	-31	-30	-10	8
5	-18	-12	-18	-12	-31	-30	-8.5	16
6	-19	-12	-19	-12	-32	-32	-8.2	
7	-19	-11	-19	-11	-34	-33	-6.5	4
Average	-18.9	-11.1	-18.9	-11.0	-30.7	-31.1	-7.9	43.2
Std. Dev	1.1	1.9	1.2	1.7	1.5	1.9	1.8	41.5

Table 1: Summary of thermal and mechanical displacement measurements of production modules. The last two lines give the average and standard deviations of the measurements.

## Appendix B : Reference [6] Thermal Test of VELO module

# Thermal test of LHCb VELO module 14 and a test of TPG inserts

*Gianluigi Casse, Karol Hennesey, Rolf Oldeman, Tony Smith*

May 22, 2006

The silicon sensors of the LHCb Vertex Locator (VELO) need to be cooled to sub-zero temperatures to avoid premature radiation damage. To achieve this, a cooling system based on a two-phase (liquid-gas) CO<sub>2</sub> mixture is used. The system used for the complete VELO is described in detail in [http://lhcb-vd.web.cern.ch/lhcb-vd/html/Assembly/Systems/cooling/EN0501\\_VTCS-EvaporatorTests16dec05\\_Draft.pdf](http://lhcb-vd.web.cern.ch/lhcb-vd/html/Assembly/Systems/cooling/EN0501_VTCS-EvaporatorTests16dec05_Draft.pdf).

For the module testing setup in Liverpool, a simplified system is used where no chiller is needed. Instead, liquid CO<sub>2</sub> is taken from a bottle at room temperature and cooled by evaporation. The CO<sub>2</sub> is not recycled. To achieve an effective cooling, a minimum flow of about 14liter/s (of gas at atmospheric pressure) is required. An overview of the setup is shown in Figure 1.

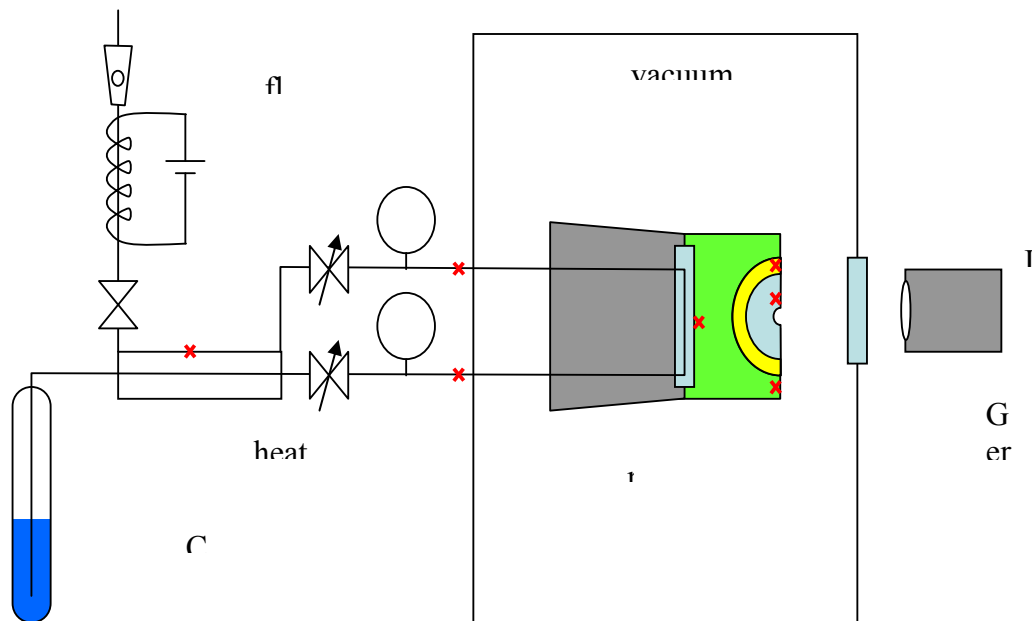


Figure 11: Schematic overview of the vacuum chamber setup for module testing in Liverpool. The red crosses indicate the positions of thermistors to measure the temperature.

The Beetle chips on the hybrid are the main source of heat on the module; about 18W per module. The other main source of heat is the environment: the vacuum tank at room temperature contributes another 6-8W per module, depending on the temperature of the module<sup>1</sup>.

The heat flow across the hybrid to the cooling block causes a temperature gradient. Here we study the temperature difference between the cooling block and several positions on the module to understand if the cooling is adequate.

For this test we used Module 14, mounted in a vacuum tank, kept at a pressure of about  $7 \times 10^{-5}$  mbar. The following characteristics of Module 14 in this setup should be noted:

- Module 14 is a so-called mechanical module with inactive sensors.
- The two thermistors on the R-side, normally mounted on the hybrid, were instead put on the phi-side; one on the silicon sensor and one on the pitch adaptors.
- All chips were bonded and powered, except the top chip on the phi side which was not functional in this test.
- The thermal connection between the cooling blocks and the hybrid was effectuated with easily removable thermal pads (3M thermally conductive interface pads, type 5509S), while the final detector will use a phase changing thermal interface material from ThermaFlo.
- Module 14 was mounted alone in the vacuum tank. Therefore it absorbs more environmental heat than the modules in the final detector configuration, most of which are surrounded by other modules cooled to sub-zero temperatures.
- The current draw on the module was 3.5A (phi-side) and 3.8A (R-side), for a voltage drop of 3.3V. This corresponds to a power consumption of  $3.3V \times 7.3A = 24.1W$ , somewhat higher than the estimated power draw of the chips.

Temperature measurements and IR pictures were taken with about 4 minute intervals, during which we increased the pressure on the valve on the outlet. The dependence between the temperatures measured on the inlet and outlet of the cooling lines are shown in Figure 2 as a function of the pressure on the outlet pipe. The temperature of the inlet and outlet are very close, and we assume here that the temperature of the cooling block is the average of the inlet and the outlet temperature. This is consistent with the cooling principle of a two-phase mixture: the heat is extracted from the evaporation of the liquid phase. The achieved temperature corresponds to the boiling point of CO<sub>2</sub>, and depends on the pressure alone. A low pressure (7 bar) corresponds to a low boiling point (-33°C) and at high pressure (13 bar) to a higher boiling point (-21°C).

---

<sup>1</sup> From Stefan's law we expect an environment contribution for a black body of  $P = \sigma A(T^4 - T_0^4)$ . Using  $\sigma = 5.67 \times 10^{-8} \text{ Wm}^{-2}\text{K}^{-4}$ ,  $A = 2 \times 0.175 \times 0.135 \text{ m}^2$ ,  $T_0 = 293 \text{ K}$ , we get for  $T = -33^\circ\text{C}$   $P = 10.9 \text{ W}$  and for  $T = -20^\circ\text{C}$   $P = 8.8 \text{ W}$ .



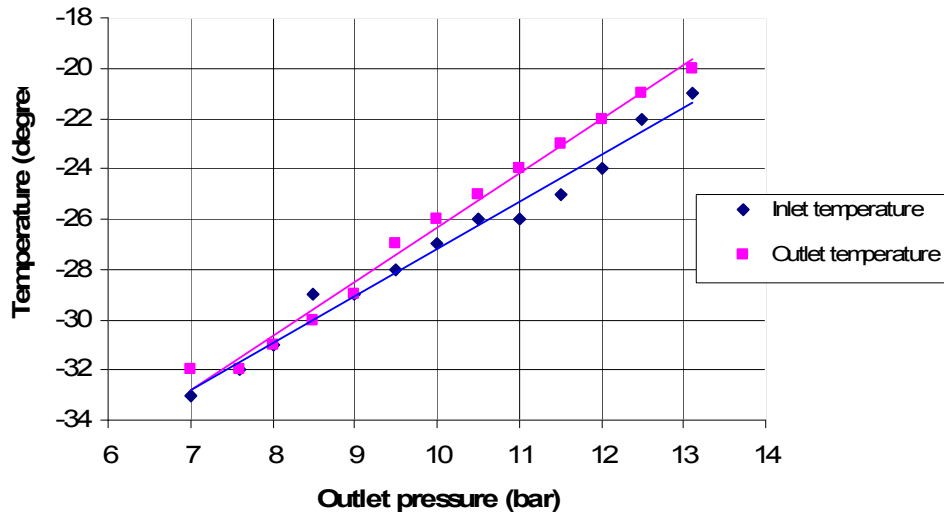


Figure 12: Relationship between the outlet pressure and the coolant temperature.

Having established the temperature of the cooling block, we can now measure the temperature difference between the four thermistors and the cooling block as a function of the coolant temperature. These measurements are summarized in Figure 3. Two of the corresponding thermal images are shown in Figures 4 and 5.

- We find a temperature drop of about 12°C between the cooling block and the 'central' hybrid position, with little dependence on the coolant temperature.
- The temperature gradient across the hybrid (centre to top) is 8°C at low temperatures, decreasing to 7°C at higher temperatures. This trend can be attributed to environmental heat absorbed by the hybrid.
- The temperature drop from the pitch adaptors to the top of the hybrid is about 2°C.
- The temperature drop from the sensor to the pitch adaptors is 3°C at low temperatures, decreasing to 1.5°C at higher temperatures.
- The total temperature difference between the sensor and the cooling block ranges from 25°C at a coolant temperature of -33°C to 21.5°C at a coolant temperature of -21°C. This trend can be attributed to environmental effects.

We also performed a quick measurement on a test module. To improve the thermal contact with the cooling block, this hybrid had a few cm<sup>2</sup> of the carbon-fibre/epoxy layer removed and replaced by TPG. Instead of Beetle chips, this module had resistors mounted, which drew the same current as the beetle chips (a total of 7.2A for both sides).

The thermistors were kept at the nominal positions: 2 at the centre, one at the top (R-side) and one at the bottom of the hybrid (phi side). A scan over coolant temperatures ranging from -28 to -19 °C is shown in Figure 6. The main thing to notice is the temperature difference between the coolant and the central thermistors, which is about 11°C, not very different from Module 14. Although the fine detail (in particular the opposite sign of the slopes of the curves are not fully understood, we can make the preliminary conclusions that the effect of the TPG inserts in the hybrids is minimal.

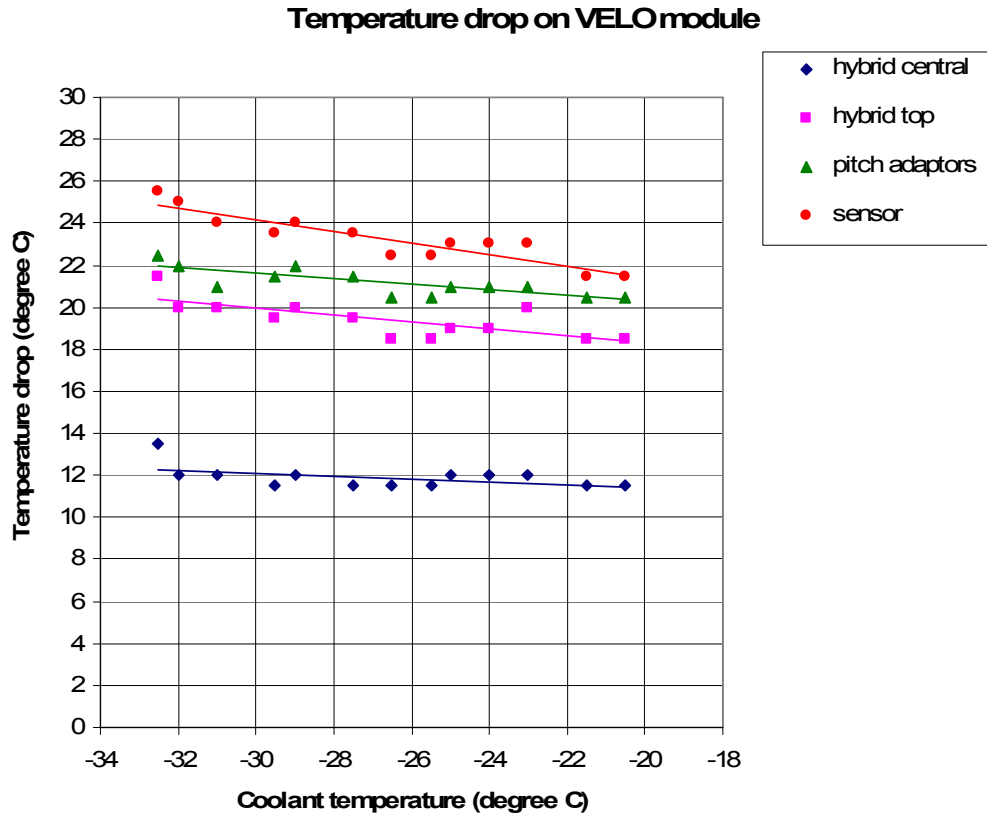


Figure 13: Temperature difference between the coolant temperature and four points on the hybrid of Module 14.

**Conclusions:**

- In the test setup, the temperature of the Silicon sensor is about 24°C higher than the coolant temperature.
- About 12°C comes from the temperature drop between the coolant and the hybrid, the other 12°C from the gradient across the hybrid.
- Using TPG inserts on the interface between the hybrid and the cooling blocks does not appear to make a significant difference.

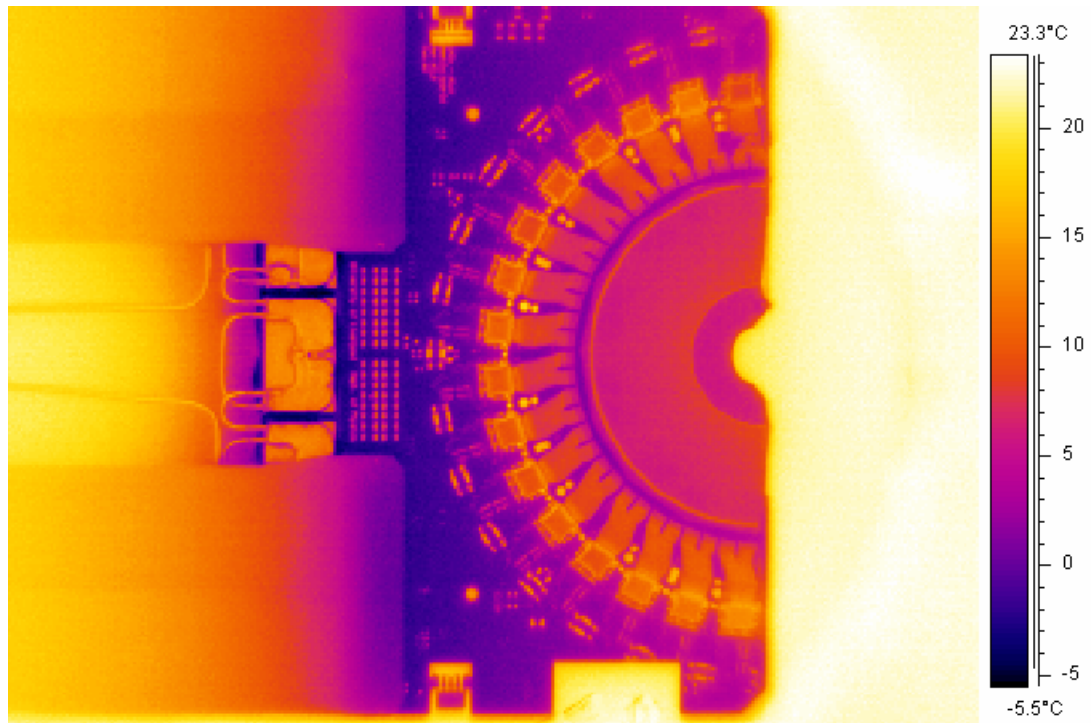


Figure 14: Thermal image of Module 14 corresponding to a coolant temperature of  $-33^{\circ}\text{C}$

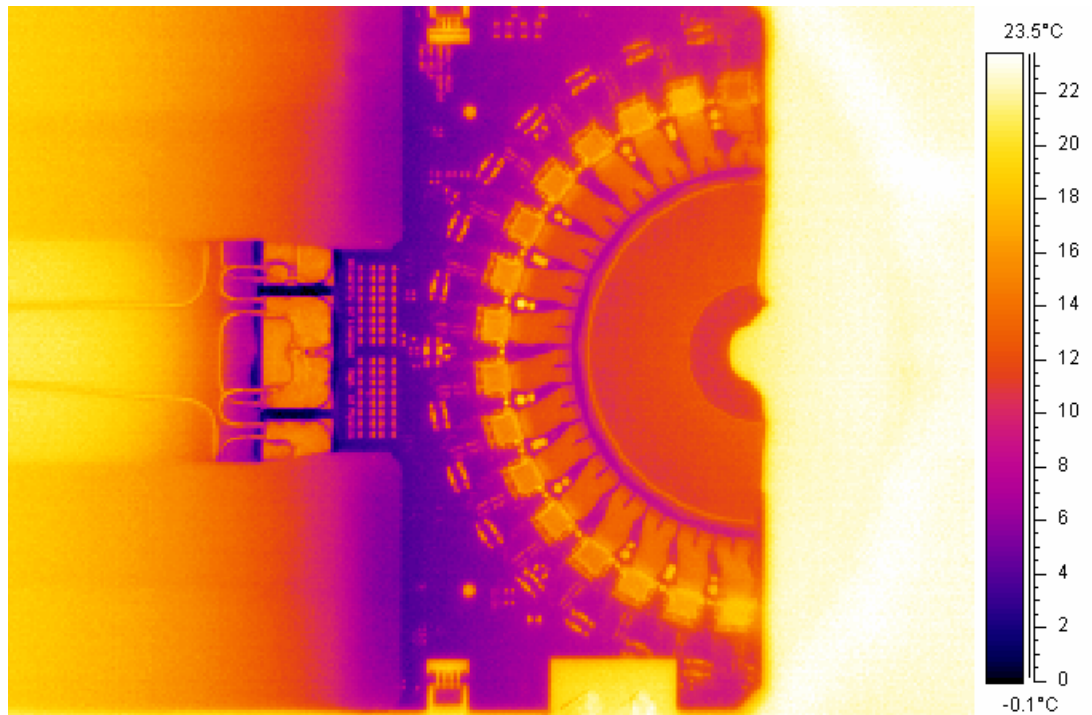


Figure 15: Thermal image of Module 14 corresponding to a coolant temperature of  $-20^{\circ}\text{C}$

## Temperature drop with TPG inserts

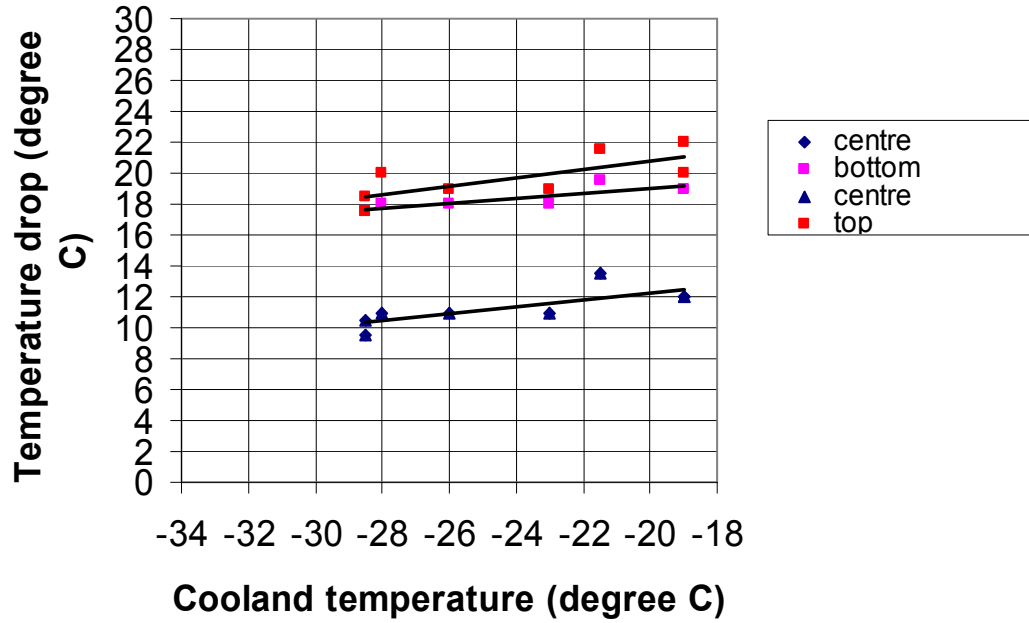


Figure 16: Thermal drop on test module with TPG inserts